Bayesian GGE biplot models applied to maize multi-environments trials

L.A. de Oliveira[1], C.P. da Silva[2], J.J. Nuvunga[2], A.Q. da Silva[1] and M. Balestre[2]

[1]Faculdade de Ciências Exatas e Tecnologia,
Universidade Federal da Grande Dourados, Dourados, MS, Brasil
[2]Departamento de Ciências Exatas,
Universidade Federal de Lavras, Lavras, MG, Brasil

Corresponding author: M. Balestre
E-mail: marciobalestre@dex.ufla.br

ABSTRACT. The additive main effects and multiplicative interaction (AMMI) and the genotype main effects and genotype x environment interaction (GGE) models stand out among the linear-bilinear models used in genotype x environment interaction studies. Despite the advantages of their use to describe genotype x environment (AMMI) or genotype and genotype x environment (GGE) interactions, these methods have known limitations that are inherent to fixed effects models, including difficulty in treating variance heterogeneity and missing data. Traditional biplots include no measure of uncertainty regarding the principal components. The present study aimed to apply the Bayesian approach to GGE biplot models and assess the implications for selecting stable and adapted genotypes. Our results demonstrated that the Bayesian approach applied to GGE models with non-informative priors was consistent with the traditional GGE biplot analysis, although the credible region incorporated into the biplot enabled distinguishing, based on probability, the performance of genotypes, and their relationships with the environments in the biplot. Those regions also

enabled the identification of groups of genotypes and environments with similar effects in terms of adaptability and stability. The relative position of genotypes and environments in biplots is highly affected by the experimental accuracy. Thus, incorporation of uncertainty in biplots is a key tool for breeders to make decisions regarding stability selection and adaptability and the definition of mega-environments.

Key words: Additive and multiplicative models; Mega-environments; Biplot; Von Mises-Fisher

INTRODUCTION

Linear-bilinear models gained prominence in the context of plant breeding and evaluation of data from multi-environment trials (METs) because they offer a range of possibilities for the analysis of genotype x environment interactions (GE). Among these models, the additive main effects and multiplicative interaction (AMMI) model and the genotype main effects and genotype x environment interaction (GGE) model, which is also known as site regression (SERG), are widely applied in genetic breeding programs and agronomic trials in general. The advantages and disadvantages of application of these methods have been extensively discussed in literature (Smith et al., 2001; Gauch, 2006; Yan and Tinker, 2006; Yan et al., 2007; Gauch et al., 2008; Balestre et al., 2009).

An interesting aspect in the study of these models is the graphical representation of the pattern of GE or GGE interaction. Such representation was originally proposed by Gabriel (1971) and was termed "biplot analysis" because it only considers the first two terms of the multiplicative model. Biplot analysis is a key step in the application of multiplicative models and is being widely and systematically used to identify patterns in MET datasets, for studying adaptability and genotypic stability, for defining mega-environments, and for other purposes regarding the evaluation of cultivars (Yan et al., 2000; Gauch, 2006). The GGE model was proposed by Yan et al. (2000) and incorporates genotype effects into the GE interaction effects of the AMMI model. It is therefore termed the GGE biplot. In this model, the overall mean and the environment effects are additive, and the genotypic effect is confounded with the multiplicative interaction component. Despite the advantages reported in the literature, like other multiplicative models, GGE has serious limitations, including difficulty in treating unbalanced or missing data and variance heterogeneity. In addition, traditional biplot analysis is merely a descriptive procedure, i.e., it includes no measure of the uncertainty regarding the genotypic and environmental scores plotted (Yan and Tinker, 2006; Yang et al., 2009). Furthermore, frequentist inference procedures in biplot analysis have been subject to criticism, whether for the assumptions regarding the distribution of the individual interaction scores required in parametric methods or for using problematic resampling procedures of non-parametric methods (Yang et al., 2009; Yan et al., 2010; Hu and Yang, 2013a; Antonio de Oliveira et al., 2015).

Alternative models based on the mixed models, including the Factor-Analytic model proposed by Piepho (1997) and Smith et al. (2001) and SERG suggested by Burgueño et al. (2008), have known advantages relative to the fixed effects models because they have more flexibility in modeling the missing data and in treating the variance heterogeneity. However,

even for these models, it is unclear how parametric confidence regions may be incorporated into the biplots (Crossa et al., 2011). These models usually consider the genotypes and interaction effects as random, whereas the environment effect is fixed. The assumption that genotype effects are random is advocated by several researchers and is a point of disagreement that has widely been discussed in the literature (Piepho, 1997; Smith et al., 2001; Crossa et al., 2006; Kelly et al., 2007).

The methods listed above are based on the frequentist approach of analysis of variance or mixed models. An alternative to analyze MET data was proposed by Viele and Srinivasan (2000), who adopted a Bayesian approach for the AMMI model. They demonstrated how to use Markov Chain Monte Carlo (MCMC) methods for performing the sampling of linear and bilinear model parameters, especially those that describe the GE interaction, whose support for conditional posterior distributions is not trivial. Subsequently, theoretical and practical questions regarding this approach were analyzed by Liu (2001), who derived a set of conditional posterior distributions, thus reducing the computational cost of the model and further stabilizing the algorithms. These studies were recently resumed and further developed by Crossa et al. (2011), Antonio de Oliveira et al. (2015), and Josse et al. (2014), who incorporated credible regions into the biplots, and also by Perez-Elizalde et al. (2011), who demonstrated how historical experimental data may be used in the inference process.

The Bayesian methodology is a natural method of incorporating uncertainty into GGE graphical representations that also facilitates treating unbalanced datasets and variance heterogeneity. It enables the use of data, other than the sampling data, including kinship matrices and historical experimental data. Another advantage of this method is that it avoids choosing which parameters should be treated as fixed or random because all unknown quantities in the Bayesian context are considered uncertain, and their realizations are probabilistic and random.

The Bayesian approach applied to the AMMI model can be generalized, i.e., it may be extended to other linear-bilinear models, including the GGE, genotype regression (GREG), and the complete multiplicative model (COMM). For such purposes, some parameters must be fixed to zero and some constraints in the models must be relaxed, as noted by Liu (2001), Crossa et al. (2011), and Perez-Elizalde et al. (2011). However, applications of the Bayesian method in the literature have been limited to the AMMI model (Viele and Srinivasan, 2000; Crossa et al., 2011; Perez-Elizalde et al., 2011; Josse et al., 2014; Antonio de Oliveira et al., 2015) and the Factor-Analytic model (de los Campos and Gianola, 2007). Thus, it would be interesting to explore the advantages of Bayesian analysis for GGE biplot models and to assess its implications for the interpretation of biplots.

In this context, the present study aimed to apply the Bayesian approach to the GGE model and investigated the various aspects related to this analysis, namely the iterative sampling process, the construction of credible regions for the genotypic and environmental scores, and the possible interpretations of these regions.

MATERIAL AND METHODS

The data used in the present study was from 55 genotypes tested under nine different environments during the 2005-2006 agricultural years. The experiment was conducted in a completely randomized block design, with three replicates. The plot consisted of two 3-m-long rows with a population density of 55,000 plants per hectare after thinning. The yield of husked

ears was the variable evaluated, which was expressed as t/ha. These data were the same as those used by Antonio de Oliveira et al. (2015).

Bayesian GGE model

The classical GGE biplot model described by Yan et al. (2000) is used to describe a dataset arranged in a double-entry matrix, wherein the plot data and designs are not explicitly incorporated into the model. We modified this model, as described by Crossa et al. (2011) and Antonio de Oliveira et al. (2015), for plotting data in the present study. The proposed GGE model was defined by the following equation:

$$\boldsymbol{y} = X_1\boldsymbol{\beta} + \sum_{k=1}^{p} \lambda_k \, diag(\mathbf{Z}\boldsymbol{\alpha}_k)\mathbf{X}_2\boldsymbol{\gamma}_k + \boldsymbol{\varepsilon} \qquad \text{(Equation 1)}$$

where, **y** represents the vector that contains the phenotypic responses. The β_{lx1} vector contains the effects related to environments and blocks (confounded), and l(l = c·b) is the number of replicates, where c and b are the numbers of environments and blocks, respectively. The terms $\mathbf{X}_1$, $\mathbf{X}_2$, and $\mathbf{Z}$ represent the incidence matrices associated with β, γ_k, and α_k. The $\mathbf{X}_2$ matrix represents the sites, and in this model, its aim was to allocate the interaction effect to the plot data. The term λ_k denotes the k-th singular value, for $k = 1,\ldots,p$, and $p = \min(r-1, c)$ is the rank of the genotypes and genotype x environment interaction $GGE_{(rxc)}$ matrix. The terms λ_k, γ_k, and α_k were obtained via singular value decomposition (SVD) of the GGE matrix.

Furthermore, this model included a constraint that $\lambda_k \geq \lambda_{k+1} \geq 0$, i.e., the values should be positive and in order of descending magnitude, and also an orthonormality constraint on the singular vectors α_k and γ_k. The ε_{nx1} vector contains the effects of experimental errors, with $\boldsymbol{\varepsilon} \sim N_n(\mathbf{0}, \sigma^2 I)$.

Only the first two principal axes were considered in the biplot for the graphical evaluation of genotype adaptability and stability, thus reducing model (1) to the known GGE (or GGE2) biplot, as proposed by Yan et al. (2000). In this analytical procedure, the first principal component was related to the genotypic adaptability, whereas the second was concerned with the stability (GE interaction).

The conditional distribution of the data has a multivariate normal density distribution, i.e., $\mathbf{y}|\beta, \lambda, \alpha, \gamma, \sigma_e^2 \sim N(\mathbf{\Theta}, \mathbf{I}_n\sigma_e^2)$, where, $\mathbf{I}_n$ denotes the identity matrix of order n, $\theta = X_1\beta + \sum_{k=1}^{p} \lambda_k \, diag(Z\alpha_k)X_2\gamma_k \, and \, \sigma_e^2$ denotes the residual variance.

Prior distributions and conditional posterior distributions of the GGE model parameters

The prior distribution of the environment effects plus the block effects is non-informative, i.e., Jeffreys prior, $p(\beta) = 1/\sigma = k$ (*constant*), is considered. A truncated normal distribution denoted by $\lambda_k \big| \mu_{\lambda_k}, \sigma_{\lambda_k}^2 \sim N^+(\mu_{\lambda_k}, \sigma_{\lambda_k}^2)$ and obtained by constraining positive values

of the normal distribution to values that meet the condition $\lambda_k \geq \lambda_{k+1} > 0$, considering $\sigma^2_{\lambda_k} \to \infty$, and $\mu_{\lambda_k} = 0$, was assigned to λ_k.

Uniform spherical distributions were assigned to the singular vectors γ_k and α_k (Viele and Srinivasan, 2000). Lastly, a scaled inverse chi-squared distribution was assigned to the residual variance. The known Jeffreys prior (Jeffreys, 1961), denoted by $1/\sigma^2_e$, was obtained when considering the scale parameters and zero degrees of freedom. These prior distributions were the same as those used by Antonio de Oliveira et al. (2015) for the Bayesian AMMI. The full conditional posterior distributions of the model parameters (1) were obtained from the joint posterior distribution. The likelihood function was expressed as

$$L(\boldsymbol{\theta}|\boldsymbol{y}) = \frac{1}{(2\pi)^{\frac{n}{2}} \left|\mathbf{I}\sigma^2_e\right|^{\frac{1}{2}}} exp\left\{-\frac{1}{2\sigma^2_e}(\boldsymbol{y}-\boldsymbol{\theta})^t(\boldsymbol{y}-\boldsymbol{\theta})\right\} \qquad \text{(Equation 2)}$$

The joint posterior distribution was obtained by applying the Bayes' theorem, which relates the prior parameter data with the likelihood function and was expressed as

$$p(\boldsymbol{\Phi}|\boldsymbol{y}) \propto p(\boldsymbol{y}|\boldsymbol{\theta},\sigma^2_e)p(\boldsymbol{\beta}|\mu_\beta,\sigma^2_\beta)p(\sigma^2_e|v,u) \times \prod_{k=1}^{p} p(\lambda_k|\mu_{\lambda_k},\sigma^2_{\lambda_k})p(\boldsymbol{\alpha_k})p(\boldsymbol{\gamma_k}) \quad \text{(Equation 3)}$$

Where $\Phi = (\beta,\alpha,\gamma,\sigma^2_e)$ and $p = \min(g-1,e)$.
Equation 3 may be rewritten using the prior data as follows:

$$p(\boldsymbol{\Phi}|\boldsymbol{y}) \propto (\sigma^2_e)^{-\frac{n}{2}} exp\left\{-\frac{1}{2\sigma^2_e}(\boldsymbol{y}-\boldsymbol{\theta})^t(\boldsymbol{y}-\boldsymbol{\theta})\right\}(\sigma^2_e)^{-1} \times \prod_{k=1}^{p} p(\lambda_k|\mu_{\lambda_k},\sigma^2_{\lambda_k})p(\boldsymbol{\alpha_k})p(\boldsymbol{\gamma_k}) \quad \text{(Equation 4)}$$

The full conditional posterior distributions for GGE model parameters were derived from Equation 4 as follows:

$$p(\boldsymbol{\beta}|\cdots) \propto exp\left\{-\frac{1}{2\sigma^2_e}\left(\boldsymbol{\beta}-(\mathbf{X}_1^t\mathbf{X}_1)^{-1}\mathbf{X}_1^t\boldsymbol{\Psi}\right)^t\mathbf{X}_1^t\mathbf{X}_1\left(\boldsymbol{\beta}-(\mathbf{X}_1^t\mathbf{X}_1)^{-1}\mathbf{X}_1^t\boldsymbol{\Psi}\right)\right\} \text{(Equation 5)}$$

$$\boldsymbol{\beta}|\ldots \sim N\left[(\mathbf{X}_1^t\mathbf{X}_1)^{-1}\mathbf{X}_1^t(\mathbf{y}-\boldsymbol{\Theta}),(\mathbf{X}_1^t\mathbf{X}_1)^{-1}\sigma^2_e\right] \qquad \text{(Equation 6)}$$

with $\psi = y - \sum_{k=1}^{p}\lambda_k diag(Z\alpha_k)X_2\gamma_k$ and $\Theta = \sum_{k=1}^{p}\lambda_k diag(Z\alpha_k)X_2\gamma_k$.

$$p(\sigma^2_e|others) \propto (\sigma^2_e)^{-\left(\frac{n}{2}+1\right)} exp\left\{-\frac{1}{2\sigma^2_e}(\boldsymbol{y}-\boldsymbol{\theta})^t(\boldsymbol{y}-\boldsymbol{\theta})\right\} \qquad \text{(Equation 7)}$$

Thus,

$$\sigma_e^2 \,|\ldots \sim inv - \chi^2[n,(\boldsymbol{y}-\boldsymbol{\theta})^t\,(\boldsymbol{y}-\boldsymbol{\theta})] \tag{Equation 8}$$

$$p(\lambda_k \,|\, others) \propto \exp\left\{-\frac{1}{2\sigma_e^2}\left[\left(\lambda_k - \left(\phi^t\phi\right)^{-1}\phi^t\Delta\right)^t\left(\phi^t\phi\right)\left(\lambda_k - \left(\phi^t\phi\right)^{-1}\phi^t\Delta\right)\right]\right\} \tag{Equation 9}$$

where $\Delta = y - X_1\beta - \sum_{k \neq k}^{p}\lambda_k diag(Z\alpha_k)X_2\gamma_k$, and $\phi = diag(Z\alpha_k)X_2\gamma_k$. The following equation was obtained after applying the constraint:

$$\lambda_k \,|\ldots \sim N^+\left[\left(\phi^t\phi\right)^{-1}\phi^t\Delta,\left(\phi^t\phi\right)^{-1}\sigma_e^2\right] \tag{Equation 10}$$

with $\lambda_i \geq \lambda_2 \ldots \geq \lambda_p \geq 0$.

Similar to the analysis by Antonio de Oliveira et al. (2015) and considering the GGE model, the full conditional posterior distributions for the singular vectors were denoted by

$$p(\boldsymbol{\alpha}_k|\cdots) \propto exp\left\{-\frac{1}{2\sigma_e^2}(\boldsymbol{y}-\mathbf{X}_1\boldsymbol{\beta}-\lambda_k\Lambda\boldsymbol{\alpha}_k-\mathbf{E})^t\,(\boldsymbol{y}-\mathbf{X}_1\boldsymbol{\beta}-\lambda_k\Lambda\boldsymbol{\alpha}_k-\mathbf{E})\right\} \tag{Equation 11}$$

With $\Lambda = diag(X_2\gamma_k)Z$ and $E = \sum_{k \neq k}^{t}\lambda_k diag(X_2\gamma_k)Z\alpha_k$

$$p(\boldsymbol{\alpha}_k\,|\cdots) \propto exp\left\{\frac{\lambda_k}{\sigma_e^2}[\alpha^t{}_k\Lambda^t\,(\boldsymbol{y}-\mathbf{X}_1\boldsymbol{\beta})]\right\} \tag{Equation 12}$$

$$p(\boldsymbol{\alpha}_k\,|\cdots) \propto exp\left\{k\alpha^t{}_k\Lambda^t(\mathbf{y}-\mathbf{X}_1\boldsymbol{\beta})\right\} \tag{Equation 13}$$

Thus, α_k has a distribution that is proportional to the Von Mises-Fisher distribution, $p(\alpha_k|\ldots) \sim VMF\left[k,\mu_{\alpha_k}\right]$, with directional mean and concentration parameter proportional to $k = \dfrac{\lambda_k}{\sigma_e^2}$ and $\mu_{\alpha_k} = \Lambda^t(y-X_1\beta)$, respectively.

Similarly, γ_k has a full conditional posterior distribution that is proportional to the Von Mises-Fisher distribution $p(\gamma_k|\ldots) \sim VMF\left[k,\mu_{\gamma_k}\right]$, with $\mu_{\gamma_k} = \Omega^t(y-X_1\beta)$ and $\Omega = diag(Z\alpha_k)X_2$.

Samples of singular vectors and the difference between GGE and Bayesian AMMI

The samples for the parameter inference process were collected using the Gibbs sampler because all the full conditional posterior distributions were known and enabled direct sampling. The steps for the iterative process were similar to those used by Antonio de Oliveira et al. (2015), although, herein, the main effect of genotypes confounded with the interaction required no update, and environmental singular vectors had no orthogonality constraint on the vector of ones (1_{ex1}). A degree of freedom was gained over that with the AMMI model because the GE matrix rank was min (g - 1, e - 1), and the GGE matrix rank was min (g -1, e).

Given the orthonormality constraint, the sampling of singular vectors was performed in the corrected space, and the vectors generated from the Von Mises-Fisher distributions using an auxiliary variable were represented in the correct space through a linear transformation (Viele and Srinivasan, 2000; Antonio de Oliveira et al., 2015). The singular vector α_k should be orthogonal to the other p - 1 vectors $\alpha_k (\mathrm{A}_{-\alpha_k})$ and the vector $\left(1_{gx1}\right)$. Thus, there was an H_k matrix whose columns formed a set of orthonormal vectors that were orthogonal to the vector $\left(1_{gx1}\right)$ and $A_{-\alpha_k}$. The auxiliary variable α_k^* was used to sample the coordinates of vectors in the corrected space (free of the orthogonality constraint). The linear transformation, $\alpha_k^* = H_k^t \alpha_k$, as proposed by Liu (2001), is a bijective function; therefore, the random vectors may be transformed into R^{n-s}, one by one, in the same vector in R^n (for n = g or n = e), where, S represents a subspace that contains the singular vectors that are orthogonal to the generated vector. $\boldsymbol{\alpha}_k^t \mathbf{H}_k \mathbf{H}_k^t = \boldsymbol{\alpha}_k^t$ is required to obtain the full conditional posterior distribution of α_k^*, which is given by

$$p(\boldsymbol{\alpha}_k \mid \cdots) \propto exp\left\{\frac{\lambda_k}{\sigma_e^2}[\boldsymbol{\alpha}_k^t \mathbf{H}^t \mathbf{H}_k^t \boldsymbol{\mu}_{\alpha_k}]\right\} \qquad \text{(Equation 14)}$$

The equation below was obtained when conveniently multiplying and dividing the part of Equation 14 between the curly brackets by $c_k = \sqrt{\mu_{ak}^t H_k H_k^t \mu_{\alpha_k}}$:

$$p(\boldsymbol{\alpha}_k^* \mid \cdots) \propto exp\left\{\frac{c_k \lambda_k}{\sigma_e^2}\left(\boldsymbol{\alpha}_k^*\right)^t \boldsymbol{\mu}_{\alpha_k}\right\} \qquad \text{(Equation 15)}$$

with $\tilde{\mu}_{\alpha_k} = c_k^{-1} H_k^t \mu_{\alpha_k}$. Thus, α_k^* had a Von Mises-Fisher distribution, which was denoted by $VFM(\dot{r} - s, \dot{k}_k, \ddot{\mu}_{\alpha_k})$, on the unit sphere S_{r-s} and was expressed as follows:

$$\boldsymbol{\alpha}_k^* \mid \cdots \sim VMF\left\{r - s, \frac{c_k \lambda_k}{\sigma_e^2}, \boldsymbol{\mu}_{\alpha_k}\right\} \qquad \text{(Equation 16)}$$

Performing the inverse transformation given by $\alpha_k = H_k \alpha_k^*$ was sufficient to obtain the genotype singular vector in the correct subspace.

γ_k^* was obtained through calculations similar to those performed for α_k such that $\gamma_k^* = R_k^t \gamma_k$. Thus, γ_k^* had a Von Mises-Fisher distribution in the corrected subspace, c - s, i.e.,

$VFM(r-s,k_k,\tilde{\mu}_{\alpha_k})$ was given by

$$p(\boldsymbol{\gamma}_k^* \mid \cdots) \propto exp\left\{\frac{d_k \lambda_k}{\sigma_e^2}\left(\boldsymbol{\gamma}_k^*\right)^t \boldsymbol{\mu}_{\gamma_k}\right\} \qquad \text{(Equation 17)}$$

where, $\tilde{\mu}_{\gamma_k} = d_k^{-1} R_k^t \mu_{\gamma_k}$, $d_k = \sqrt{\mu_{\gamma_k}^t R_k R_k^t \mu_{\gamma_k}}$, and the R_k matrix had columns that were orthonormal and orthogonal to the $D_{-\gamma_k}$ vectors. The inverse transformation was obtained by $\gamma_k = R_k \gamma_k^*$.

As already mentioned above, for environmental singular vectors, there was no orthogonality constraint regarding the vector (1_{ex1}), i.e., each γ_k was orthogonal to p - 1 vectors in R^e, whereas each α_k was orthogonal to p in R^g. The latter assumption is crucial for the Bayesian GGE approach.

The convergence of Markov chains obtained using the Gibbs sampler was monitored using the criteria of Raftery and Lewis (1992) and Gelman and Rubin (1992). The residual variance and singular value estimates were obtained using the posterior means for the MCMC sample generated. The same did not occur for the singular vectors in which posterior means did not satisfy the unit norm and orthogonality constraints, thus requiring transformation into matrices formed by the means of coordinates of the resulting vectors obtained by the Markov chains. The method proposed by Liu (2001) was used for that purpose.

The highest posterior density (HPD) credible regions for the model parameters were obtained using the method proposed by Chen and Shao (1999) and were implemented using the statistical package Bayesian Output Analysis (BOA) available in the R software package (R Development Core Team, 2013).

Credible regions for the scores $(\lambda_1^{1/2}\alpha_{i1}, \lambda_2^{1/2}\alpha_{i2})$ and $(\lambda_1^{1/2}\gamma_{j1}, \lambda_2^{1/2}\gamma_{j2})$, with $i = \{1,...,55\}$ and $j = \{1,...,9\}$, were incorporated into the biplot using the Euclidean distances method, as reported in Ooms (2009) and Antonio de Oliveira et al. (2015). As previously reported, the first two terms in the bilinear model (1) were considered for graphic evaluation of the genotype adaptability and stability. The interpretations were performed by observing the overlap between the credible regions of the genotypic and environmental scores. Genotypes and environments whose regions for the biplot scores intersected each other were considered similar or homogeneous groups.

RESULTS

GGE in the frequentist context

The frequentist GGE analysis indicated that the first of the eight principal components (PCs) obtained in this study, PC1, accounted for 45.54% of the G+GE effects, and the second component, PC2, accounted for 12.44% of that effect. Thus, PC1 and PC2 together explained 57.98% of the total G+GE effect. These results indicated that the first two principal components could explain a large part of the G+GE effect. However, this percentage might not be sufficient to explain the interaction pattern (Cullis et al., 2014; Smith et al., 2015).

The GGE2 biplot, which corresponded to the GGE biplot analysis shown in Figure 1, was used for the graphical representation of the pattern expressed by the first two PCs. A polygon was designed based on the genotypes located in the farthest points of Figure 1. The genotypes G35, G19, G29, G50, G47, G27, G2, and G6 were the vertices of this polygon. Considering the first two PCs (PC1 and PC2), the G6 genotype exhibited the best response to the prevailing environmental conditions during crop growth. The G4, G24, G46, and G49 genotypes might be considered the most stable and productive. In contrast, the G35, G19, G29, and G50 genotypes were the least productive because they were located far from the test environments, reflecting the fact they produced little in each environment. The G35 genotype might be considered the least stable of all the genotypes.

The mega environments may be determined by drawing lines perpendicular to the edges of the polygon. Two mega-environments were observed in the GGE biplot. The first one, which was termed mega-environment I, was formed by environments A1, A2, A3, A4, A7, A8, and A9 and included the most productive and stable genotypes. The second mega-environment contained only the environment A6.

The which-won-where pattern indicated that G6 was the best-performing genotype in the first mega-environment, and G2 exhibited the best performance in the second mega-environment (Figure 1). Although these hybrids were classified as winning genotypes based on an analysis of Figure 1, these genotypes were slightly distant from the origin, compared to the second principal component (PC2), thereby, suggesting that they were not very stable when environment 6 was included. It must also be emphasized that such an arrangement of environments and genotypes is based on a single sample; i.e., the biplot has a descriptive nature and overlooks the uncertainty regarding the plotted scores, as has been argued by several researchers (Yang et al., 2009; Hu and Yang, 2013a).
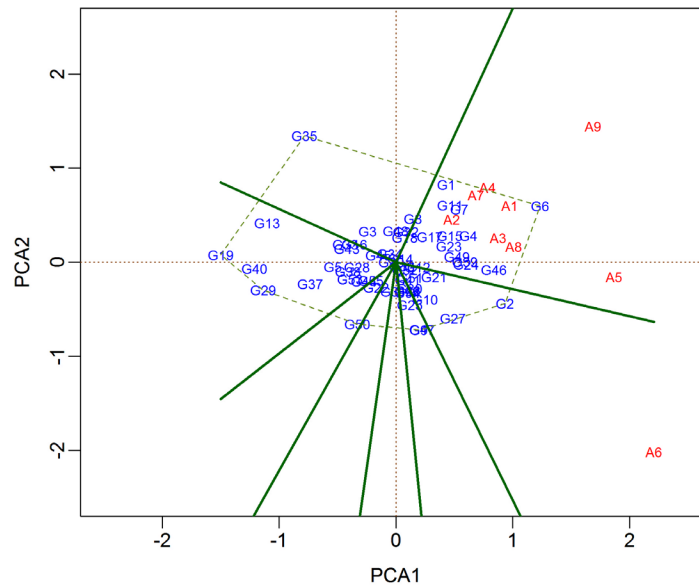

Figure 1. Biplot analysis of the GGE model, considering 55 genotypes tested in nine environments, using the frequentist approach.

The results of the Bayesian proposal for the GGE biplot model for the same dataset used in the fixed effect analysis are presented below.

Bayesian GGE approach (BGGE)

MCMC chains with 90,000 iterations were simulated for the GGE model parameters in the Bayesian analysis. The first 10,000 observations were discarded to avoid selecting samples of chains dependent on the initial state and that had not yet reached convergence. Moreover, the samples were collected performing jumps every 12 observations. The last procedure aimed at selecting uncorrelated observations. At the end of this process, samples with 6,666 observations were obtained for each parameter. The convergence of Markov chains generated using the Gibbs sampler was monitored using the criteria by Raftery and Lewis (1992) and Gelman and Rubin (1992), as specified in the Methods section. Those tests indicated good convergence for all the model parameters.

Figure 2 shows the lines of chains generated for the first three singular values and for the residual variance. As shown in the figure, the values of each chain tend to cluster around a specific value, thereby, corroborating the results of the convergence tests performed. This trend was observed for all the model parameters.
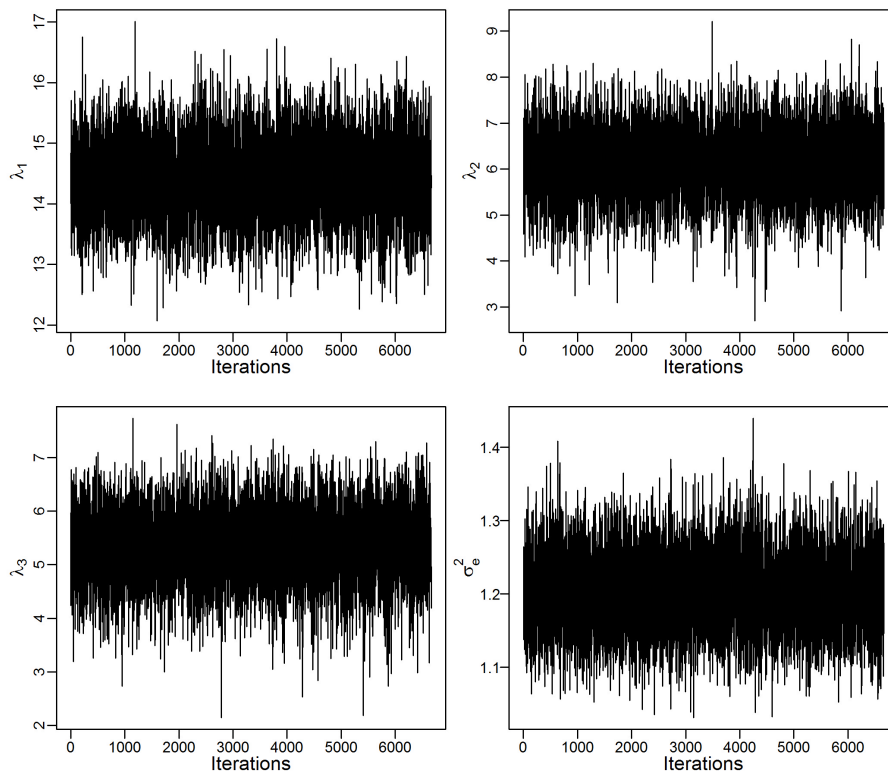

Figure 2. MCMC plots of the first three singular values and residual variance $\left(\sigma_e^2\right)$.

Figure 3 shows plots of the conditional posterior densities of singular values. The distributions move increasingly left such that the mode is increasingly close to zero, a result that agrees with the theory of principal component analysis $(\lambda_k \geq \lambda_{k+1})$.
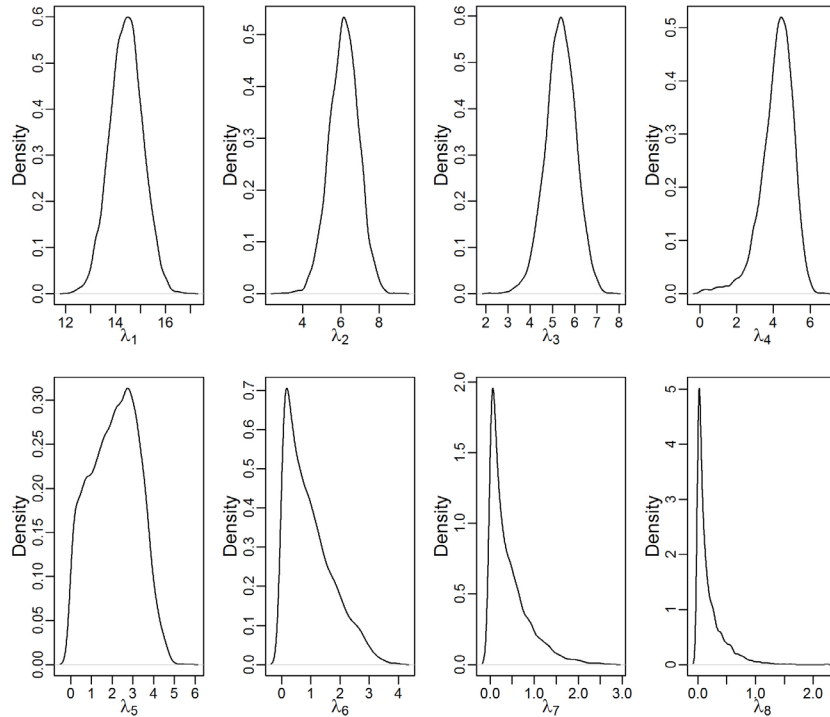

Figure 3. Posterior marginal densities of the singular values.

Moreover, the first three singular values apparently also followed a normal distribution and the distributions became increasingly asymmetrical as of the fourth singular value.

Table 1 outlines the posterior means of the singular values for the BGGE model, together with the respective HPD regions. Furthermore, Table 1 also shows ordinary least squares (OLS) estimates regarding the application of the GGE model for fixed effects (GGEF).

Table 1. Posterior mean (PM), standard deviation (SD), credible region (95% C.I., LL: Lower limit, UL: upper limit), and ordinary least squares (OLS) estimate for singular values (λ).

Parameter	MP	SD	LI	LS	OLS
λ_1	14.4286	0.6529	13.1511	15.6880	15.2471
λ_2	6.1552	0.7578	4.7017	7.6773	7.9687
λ_3	5.3594	0.6802	4.0145	6.6679	7.7909
λ_4	4.1985	0.8945	2.4342	5.7933	6.8740
λ_5	2.1103	1.1231	0.0031	3.8463	5.6920
λ_6	0.9562	0.7906	<0.0001	2.5396	5.4507
λ_7	0.4192	0.4431	<0.0001	1.3332	5.1155
λ_8	0.1888	0.2377	<0.0001	0.6894	3.1990

The values predicted by the posterior distributions were smaller than the OLS estimates. It should also be noted that the first two axes accounted for 67% of the variation, whereas the first two PCs explained 57.98% of the variation in the fixed effects model. The correlation between the first main axis and the genotypic effects was 97.80%. That result enables one to conclude that the genotypic effect was markedly absorbed by the first main axis in the BGGE model. This means that the information regarding genotypic adaptability is embedded in the first singular value, which enables a better interpretation of the biplot representation. A value of 1.201, with a posterior credible interval of (1.099; 1.307) at the 95% probability level, was obtained for the posterior mean of residual variance (σ_e^2).

Point estimates and credible regions of the genotypic and environmental singular vector coordinates regarding the first two axes are presented in **S1 Table**. This Table also indicates that the values of posterior estimates were very close to the least squares estimates of the genotypic and environmental vector coordinates for the first axis. A greater difference was observed between the posterior means and OLS estimates for the second axis.

The posterior densities of the first genotypic and environmental scores for the first main axes are shown in Figure 4. The respective densities have apparent symmetry and bell shapes, which suggest that they obey a normal distribution. This fact was observed for all the genotypic and environmental scores for the first two PCs, which leads to the conjecture that the bivariate distributions of scores on the biplot regarding the first two individual axes may be adequately approximated by the normal distribution for this dataset.
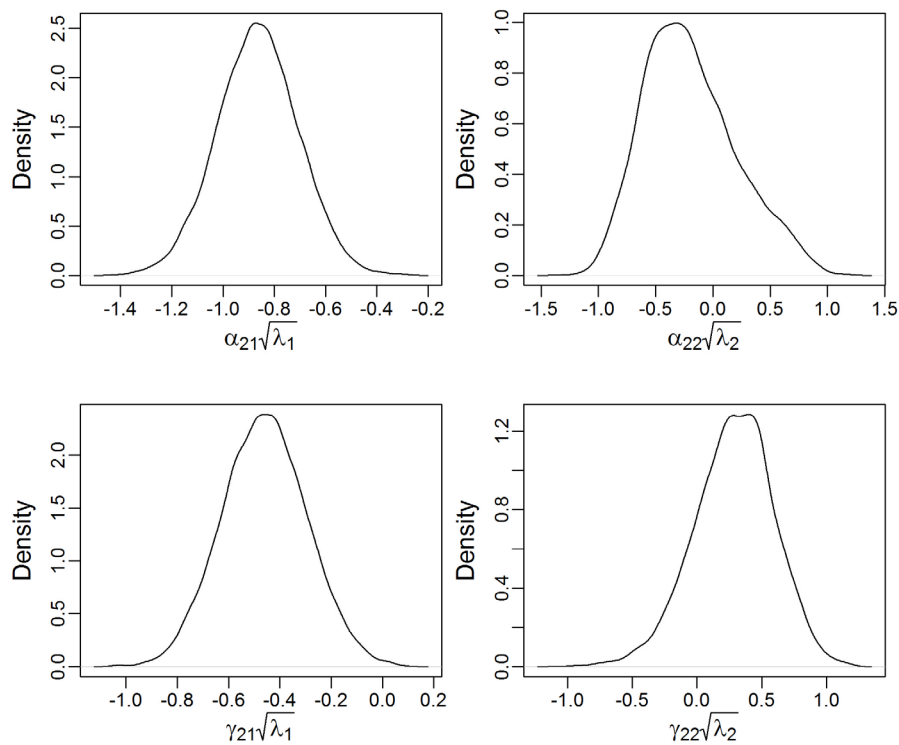

Figure 4. Posterior marginal densities of the first genotypic and environmental scores for the first two main axes.

Figure 5 shows the biplot representation, which was obtained by exclusively considering the first two axes of the GGE model (GGE2). This graphical representation consisted of the posterior means of genotypic and environmental scores for the first two PCs. This "posterior biplot" clearly maintained the same pattern as the traditional biplot, as shown in Figure 1, which indicated that the Bayesian approach captured the original pattern of the dataset.
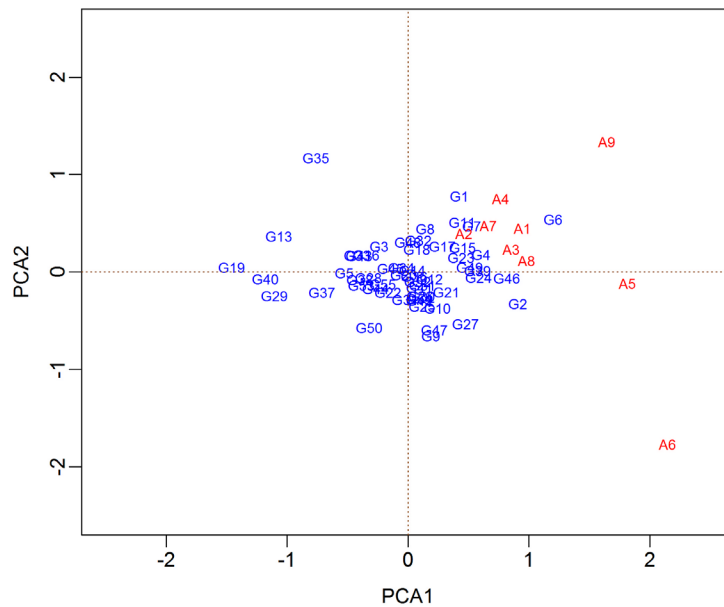

Figure 5. Biplot constructed using the posterior means for the first two main axes.

The bivariate empirical 95% credible regions obtained for each genotypic score are shown in Figure 6. These intervals were constructed using the method reported by Antonio de Oliveira et al. (2015), although the interpretation was different because we considered the scores related to genotypes and interaction (GGE pattern), i.e., the genotype effect was confounded with the interaction effect. Only genotypes at the polygon vertices, with their respective credible regions, and the ones whose regions for the scores did not include the origin (0,0), were plotted to achieve greater simplicity and ease of visualization. The graphical visualization shows that the genotypes at the vertices were the same as those observed in the GGE biplot for fixed effects.

The GGE biplot, or GGE2 biplot, with the posterior means of genotypic and environmental scores and 95% credible regions, is shown in Figure 7. Following the standard interpretation of this graphical tool, eight perpendicular line segments were drawn next to the polygon, starting at the origin. Different subsets of environments and genotypes may be observed in these sectors. The genotype vertices of the polygon are considered to be those with the best performance compared with the environments in each which-won-where sector. However, interpretations should be made considering the 95% credible regions of the scores. It should also be noted that all the environmental sectors were located to the right of the vertical axis, in agreement with the results reported by Yan et al. (2000).
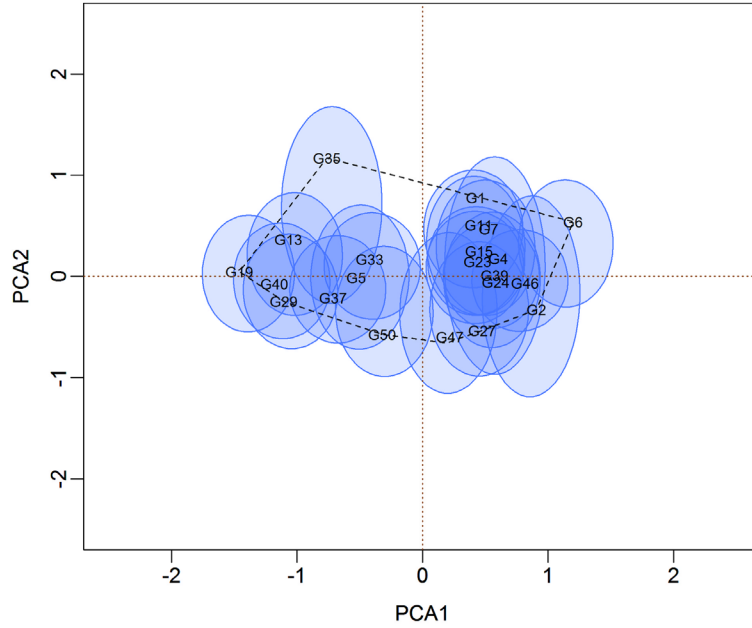
Figure 6. 95% credible regions for the genotypes of the polygon vertices and genotypes whose credible regions do not include the origin.
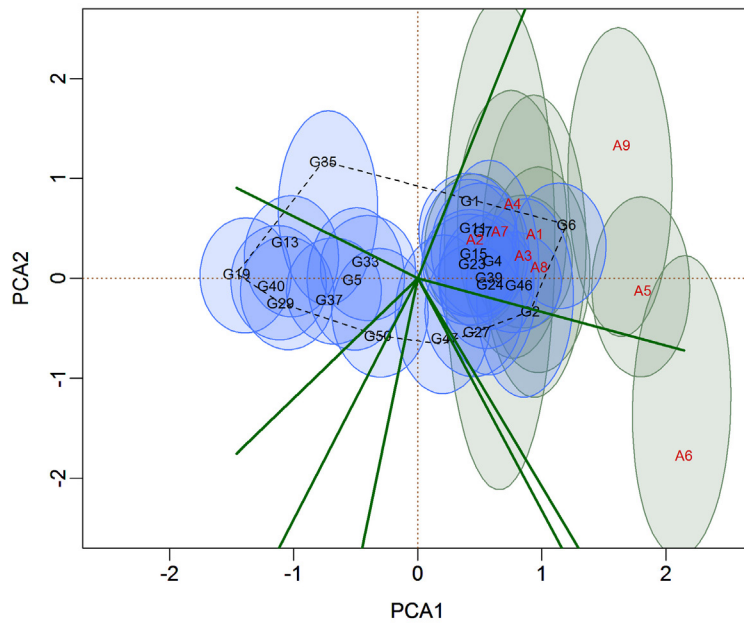

Figure 7. 95% credible regions for the genotypes of the polygon vertices and the genotypes and environments whose credible regions do not include the origin.

This plot showed higher overlap of the credible regions among the environments A1, A2, A3, A4, and A7, which indicates that they might have had similar effects regarding the interaction and could, therefore, be considered a homogeneous cluster, although increased variability was observed in the values of environment A7. Environments A9 and A5 had considerable overlap, suggesting effects similar to one another, although some overlap of credible regions of the group, as emphasized above, was observed. Environment A6 had different levels of overlap with A9 and A5. However, it was apparently most different from the other environments and was also the environment that contributed most to the interaction.

As emphasized above, the configuration of the Bayesian GGE biplot with the posterior means maintained the same pattern as the frequentist approach. However, no uncertainty was considered in the traditional method (Figure 1). As performed for the environments, genotypes whose bivariate credible regions for the scores intersect each other may be considered similar in terms of adaptability and stability. Three clusters may be defined using this criterion: i) those on the left of the vertical axis that, because they are distant from the environmental scores, exhibit lower performance in terms of all scores, i.e., they can be discarded by the genetic breeder upon simple graphical analysis and with a known type I error rate; ii) those on the right of the same axis, whose credible regions of scores overlap at different levels; iii) genotypes whose credible regions include the origin at 95% probability, which cannot be considered unstable and do not significantly deviate from the overall mean. As shown in the figure, the G50 and G45 genotypes belonged to group iii, although they were located at the polygon vertices. We could extend this criterion to others scenarios, including the following: (i) genotypes whose credible ellipses covered intervals $(0 < PC_1, 0 < PC_2)$ and $(0 < PC_1, 0 < PC_2)$ could be classified as poorly adapted and of low homeostasis; (ii) $(0 < PC_1, 0 < PC_2)$ poorly adapted genotypes, albeit not unstable at 5%; (iii) $(0 < PC_1, 0 < PC_2)$ genotypes with no difference from the overall mean and not unstable; (iv) $(0 = PC_1, PC_2 > 0 \text{ V } PC_2 < 0)$ genotypes with no difference from the overall mean and unstable; (v) $(PC_1 > 0, PC_2 > 0 \text{ V } PC_2 < 0)$ genotypes with high general adaptability, albeit with little overall stability (or those that were stable or recommended for a particular mega-environment); and (vi) $(PC_1 > 0, PC_2 = 0)$ genotypes with high yield and wide adaptation.

Figure 8 shows the direction of genotypes whose credible interval did not include the origin in PC_1. Thus, as shown in the figure, we could separate clusters of genotypes that differed from each other in terms of adaptability. Conversely, we observed that no genotypes differed from each other in terms of stability. Regarding the formation of mega-environments, we observed that the two mega-environments formed by the biplot analysis of the data were not consistent, given the high overlap of the intervals of the environments between the two clusters. Thus, there was no evidence of more than one mega-environment.

DISCUSSION

The present study aimed at applying a Bayesian approach for the GGE (or SERG) model, which is obtained from the general linear-bilinear model (GLBM) when the environment effects are removed (Yang et al., 2009). Although some studies using Bayesian inference associated with multiplicative models have been reported, they have been restricted to the application of the AMMI model only, and no study that associates Bayesian inference with other linear-bilinear models, especially with the GGE (or SERG) model, has been reported to date.
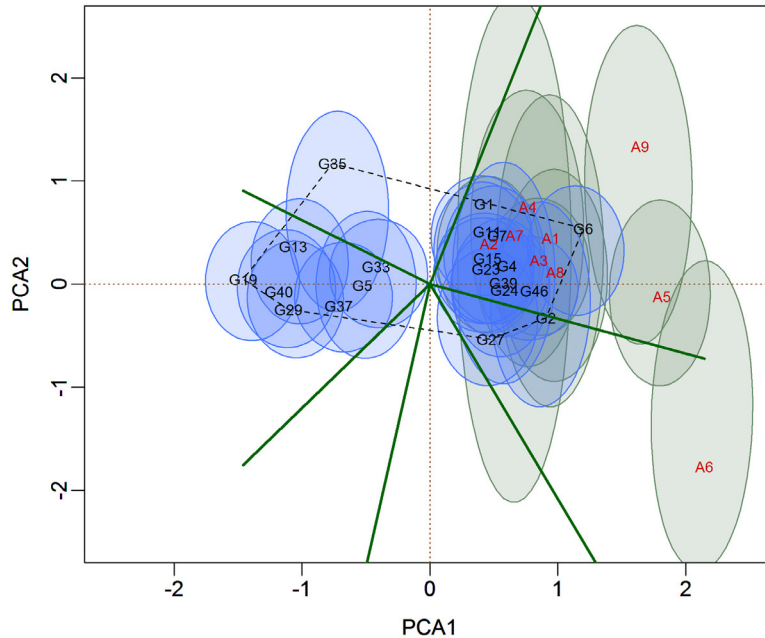
Figure 8. Bivariate 95% credible regions that do not include the origin for genotypic and environmental scores.

We assigned non-informative prior distributions, similar to those used by Crossa et al. (2011), to all parameters of the GGE model. The efficacy of the approach reported in this study was confirmed based on the results obtained because the pattern of the biplot graphical representation of the traditional analysis was conserved by the biplot consisting of posterior means (Figure 5). Furthermore, as indicated in **S1 Table**, the values obtained for posterior means of the first axis coordinates were very close to the least squares estimates of the fixed effects model, which also indicated that our approach with non-informative prior distributions was similar to the traditional GGE approach. Greater differences between the Bayesian and OLS estimates were observed for the second and remaining subsequent axes. This fact may have resulted from the shrinkage effect of the estimates of singular values, which is clear from the second axis because the credible region for λ_2 did not include the value of the OLS estimate (**S1 Table**). As noted by Liu (2001), the estimates of the singular vector coordinates are apparently affected by the magnitude of the λ_K values.

Even when assigning non-informative prior distributions to all parameters, the maximum a posteriori probability (MAP) estimates of singular values were shrunken when compared with the OLS estimates of the fixed effects GGE. That shrinkage became increasingly more pronounced for higher-order singular values. This fact has been observed in studies with the Bayesian AMMI model (Crossa et al., 2011; Perez-Elizalde et al., 2011; Antonio de Oliveira et al., 2015; da Silva et al., 2015). Indeed, stronger shrinkage effect should be expected when assigning specific prior distributions to variance components of singular values, thereby shrinking the estimate of singular values related to the axes of higher order until zero and leading to more pronounced predictions for singular values associated with the

first axes. This result was clearly observed in the derivations of Bayesian AMMI shrinkage described by da Silva et al. (2015).

Other aspects may also be highlighted here and agree with the approaches using "Bayesian AMMI" that have been previously presented in the literature. First, the standard deviations for the first axis increased up to λ_5, which was obviously reflected in the HPD credible regions. This result agrees with the theory of principal component analysis, in which the first axes are estimated most accurately (Crossa et al., 2011; Antonio de Oliveira et al., 2015). However, the standard deviation values decreased starting at λ_6. This decrease surely resulted from the shrinkage effect, which became more pronounced as of the sixth singular value, i.e., there was little variation around a very low value, thus, indicating that the latter axes did not have a significant contribution to explaining the *GGE* pattern. The same trend was observed for the singular vector coordinates. Vectors related to the first singular values had lower variance - as indicated by the standard deviation values, which were greater than vector coordinates associated with higher-order axes. That fact, as emphasized by Antonio de Oliveira et al. (2015), may be explained by the larger magnitude of the first singular values because the vector coordinates were generated from Von Mises-Fisher distributions, for which a higher value of the concentration parameter indicates that points are more clustered around the directional mean.

Elliptical 95% credible regions were also constructed for the GGE2 biplot. These regions are based on the Euclidean distances of the points from the center of the distributions of scores, similar to the regions reported by Antonio de Oliveira et al. (2015). Crossa et al. (2011) and Perez-Elizalde et al. (2011) also reported HPD credible regions for genotypic and environmental scores, which were used to separate homogeneous groups of genotypes and environments based on the interaction effect. Methods for obtaining confidence regions, free of theoretical assumptions regarding the distribution of scores, may also be found in the report of Hu and Yang (2013b).

It is noteworthy that Bayesian inference offers a flexible and parametric method for inference of the biplot, based on the joint posterior distribution, unlike parametric frequentist methods (Denis and Gower, 1996), which are difficult to extend to more complex models and require restrictive assumptions regarding the distribution of individual scores (Yang et al., 2009; Hu and Yang, 2013a). Component tests based on the F distribution may offer a reasonable fit to the first singular values. However, the normality assumption is difficult to satisfy for the highest singular values, as shown in Figure 3.

Furthermore, there are known limitations of fixed effects models, including their difficulty in treating unbalanced data and variance heterogeneity - although some methods have been suggested to circumvent such difficulties using additional procedures to impute missing values, namely, the expectation-maximization (EM)-AMMI by Gauch and Zobel (1990) and methods based on cross-validation (Dias and Krzanowski, 2003). Rodrigues et al. (2014), for example, proposed a weighted algorithm of decomposition of singular values to treat variance heterogeneity, the weighted AMMI (W-AMMI), which may be considered an alternative to mixed model analyses and may be applied to a wide range of situations. A critique of biplot methods is their descriptive and non-inferential nature, i.e., uncertainty is not considered in the plots that described the GE or G+GE pattern. Accordingly, Yang et al. (2009) voiced a strong critique regarding conclusions about the biplot and suggested using non-parametric methods, including bootstrapping, as inference tools and incorporating confidence regions

into biplots. The approach suggested by Yang et al. (2009) was subsequently improved using a bidirectional bootstrapping procedure with the Procrustes rotation developed by Hu and Yang (2013a), which was motivated by the fact that the singular value decomposition of a matrix is not unique. However, this method is susceptible to criticism regarding the computationally intensive resampling of the rows and columns of GGE matrices. The main problem is that score positions in a biplot are mutually defined, and the signs and values become meaningless when genotypic scores are randomly separated from environmental scores by the resampling process, thus destroying the original data pattern (Yan et al., 2010). Our results do not invalidate the use of the GGE biplot as an analytical tool. On the contrary, they demonstrate that the GGE Biplot may be a powerful tool for genetic breeders, provided that good experimental accuracy is achieved, which will consequently affect the range of the credible interval and the decision-making process.

Another discussion that naturally emerges regards the interpretation of confidence regions in biplots. When using the interpretations present in the literature (Crossa et al., 2011; Perez-Elizalde et al., 2011; Hu and Yang, 2013a; de Oliveira et al., 2015), one can observe that the "which-won-where" pattern, which is commonly used in traditional analysis, was not observed at 95% credibility. Another fact to be highlighted is the overlapping credible regions, which preclude differentiating the effects of genotypes that belong to the two mega-environments found in the traditional method. Furthermore, different levels of overlap are observed for the credible regions of environmental scores, thus complicating the separation of groups. However, experience and common sense of researchers may help them differentiate between homogeneous groups of genotypes and mega-environments. Denis and Gower (1996), for example, differentiated homogeneous groups of genotypes and environments, even when a considerable degree of overlap existed among the confidence regions.

Nonetheless, research studies aimed at more consistent interpretations of inference procedures for biplot analysis are necessary. The polygon shown in Figure 7, along with the perpendicular lines and credible regions, for example, refers to posterior means. However, formation of a different polygon would occur for each interaction. Thus, using a static polygon to interpret patterns through credible regions does not seem reasonable. Hence, the procedure used herein only consisted in observing the overlap between regions to draw conclusions from the MET dataset of the original GGE. The same observation may be extended to the perpendicular lines that define mega-environments.

The key to implementing the Bayesian GGE biplot is its essential difference from the AMMI model; as stated in the methods section, this approach is based on the constraint that singular vectors are orthogonal to the vector 1_{nx1} (for n = g or n = e). The effects add up to zero in the rows and columns of the GE interaction matrix, to be decomposed in the AMMI method. Thus, that the rank is given by $p = \min (r$ -1$, c$ - 1$)$. For the genotype and GE effects matrix (GGE), the effects in rows still add up to zero, although the effects in the columns do not. As a result, the new rank of this matrix is $p = \min (r - 1, c)$, i.e., the constraint that environmental singular vectors must be orthogonal to the vector 1_{ex1} is not present in the GGE model. Thus, for a successful Bayesian GGE, we cannot simply remove the effects of the means and environments from the AMMI model and confound the effects of interaction and genotypes to obtain the approach described in the present study. These details should be considered in the MCMC sampling process, such that the method may be correctly applied.

The main question is whether the uncertainty present in the biplot requires a GGE

analysis as complex as that reported in the present study. The authors' answer to that question is yes, because incorporation of uncertainty is a consequence of the Bayesian approach and not an end. Put otherwise, the Bayesian GGE model enables one to treat unbalanced data and variance heterogeneity, among other advantages, which, thus far, has only been effectively exploited in mixed models with factor analytic structures. Kelly et al. (2007) and Burgueño et al. (2008) demonstrated that despite the superiority of factor analytic models and their ability to incorporate kinship and variance heterogeneity, it is not easy to use such models because of the need to impose constraints to ensure that the solutions are within the parameter space, as determined by Thompson et al. (2003). de los Campos and Gianola (2007) introduced the Bayesian approach of the AF model, in which the constraints necessary in its frequentist version are unnecessary because the use of prior data eliminates those constraints. However, this model is not easily interpreted or applied because Bayesian factor analysis is quite complex.

Accordingly, modeling variance heterogeneity becomes easily implemented in the Bayesian GGE when assuming an inverted Wishart. Because our approach claims the same features as AF models, a possible addition to those models regards the number of parameters to be estimated, which are always expressed as a function of min(g-1, e). For example, if GGE2 is chosen, the researcher will need to resort to six partial derivatives of conditional distribution (3) or 3[min(g-1, e)] for any number of terms to obtain all the GGE parameters, not (e(e-1)/2), for example, as required in AF models, in addition to several constraints that must be imposed to ensure a single solution for the load matrix (Smith et al., 2001; Meyer, 2009). Furthermore, all partial derivatives have closed-form solutions, and Heywood cases for singular values may be mitigated if the prior distribution is non-informative. Thus, the derivation of posterior approach for conditional distributions reported in this study may be easily applied and direct obtainment of the MAP rather than numerical integration of the conditional distributions may render the approach more efficient compared with the algorithms reported in mixed models with factor analytic structure. This is a topic of ongoing research. Another advantage of GGE analysis over AF is that the model interpretation is direct, with no need for arrangements, unlike the AF interpretation from the GGE standpoint, if two factor loadings are considered and the G effects are confounded with the GE (Burgueño et al, 2008; Stefanova and Burchiell, 2010).

The dataset used in the present study was the same as used by Antonio de Oliveira et al. (2015) and, although some small differences were observed, a similar pattern regarding the best genotypes in terms of yield and those with the poorest yields was observed. As already emphasized, the Bayesian method offers several advantages relative to the frequentist methods, either because of the flexibility in treating heteroscedastic datasets as well as unbalanced data or because it allows incorporating additional data into the analysis, thus, improving the inference process. Because GGE analysis has been systematically used to draw conclusions and make important decisions, there is a need to construct inference procedures based on biplots to ensure that the results obtained are critical rather than merely descriptive. Accordingly, the method reported, herein, is quite promising. New GGE approaches that consider specific priors for the parameters will certainly be a topic of future research.

Conflicts of interest

The authors declare no conflict of interest.

REFERENCES

Antonio de Oliveira L, da Silva CP, Nuvunga JJ, da Silva AQ, et al. (2015). Credible intervals for genotypic and environmental scores in the AMMI model with random effects for genotype. *Crop Sci.* 55: 465-476. http://dx.doi.org/10.2135/cropsci2014.05.0369

Balestre M, Souza JC, Von Pinho RG, de Oliveira RL, et al. (2009). Yield stability and adaptability of maize hybrids based on GGE biplot analysis characteristics. *Crop Breed. Appl. Biotechnol.* 9: 219-228. http://dx.doi.org/10.12702/1984-7033.v09n03a03

Burgueño J, Crossa J, Cornelius PL and Yang RC (2008). Using factor analytic models for joining environments and genotypes without crossover genotype x environment interaction. *Crop Sci.* 48: 1291-1305. http://dx.doi.org/10.2135/cropsci2007.11.0632

Chen MH and Shao QM (1999). Monte Carlo estimation of Bayesian credible and HPD intervals. *J. Comput. Graph. Stat.* 8: 69-92.

Crossa J, Burgueno J, Cornelius PL, McLaren G, et al. (2006). Modeling genotype x environment interaction using additive genetic covariances of relatives for predicting breeding values of wheat genotypes. *Crop Sci.* 46: 1722-1733. http://dx.doi.org/10.2135/cropsci2005.11-0427

Crossa J, Elizalde SP, Jarquin D, Cotes JM, et al. (2011). Bayesian estimation of the additive main effects and multiplicative interaction model. *Crop Sci.* 51: 1458-1469 http://dx.doi.org/10.2135/cropsci2010.06.0343.

Cullis BR, Jefferson P, Thompson R and Smith AB (2014). Factor analytic and reduced animal models for the investigation of additive genotype-by-environment interaction in outcrossing plant species with application to a *Pinus radiata* breeding programme. *Theor. Appl. Genet.* 127: 2193-2210. http://dx.doi.org/10.1007/s00122-014-2373-0

da Silva CP, de Oliveira LA, Nuvunga JJ, Pamplona AKA, et al. (2015). A Bayesian shrinkage approach for AMMI models. *PLoS One* 10: e0131414 http://dx.doi.org/10.1371/journal.pone.0131414.

de los Campos G and Gianola D (2007). Factor analysis models for structuring covariance matrices of additive genetic effects: a Bayesian implementation. *Genet. Sel. Evol.* 39: 481-494. http://dx.doi.org/10.1186/1297-9686-39-5-481

Denis JB and Gower JC (1996). Asymptotic confidence regions for biadditive models: Interpreting genotype-environment interactions. *Appl. Stat.* 45: 479-493 http://dx.doi.org/10.2307/2986069.

Dias CTS and Krzanowski WJ (2003). Model selection and cross validation in additive main effects and multiplicative interaction models. *Crop Sci.* 43: 865-873 http://dx.doi.org/10.2135/cropsci2003.8650.

Gabriel KR (1971). The biplot graphic display of matrices with application to principal components analysis. *Biometrika* 58: 453-467 http://dx.doi.org/10.1093/biomet/58.3.453.

Gauch HG (2006). Statistical analysis of yield trials by AMMI and GGE. *Crop Sci.* 46: 1488-1500 http://dx.doi.org/10.2135/cropsci2005.07-0193.

Gauch HG and Zobel RW (1990). Imputing missing yield trial data. *Theor. Appl. Genet.* 79: 753-761. http://dx.doi.org/10.1007/BF00224240

Gauch HG, Piepho HP and Annicchiarico P (2008). Statistical analysis of yield trials by AMMI and GGE: Further considerations. *Crop Sci.* 48: 866-889 http://dx.doi.org/10.2135/cropsci2007.09.0513.

Gelman A and Rubin DB (1992). Inference from iterative simulation using multiple sequences. *Stat. Sci.* 7: 457-472. http://dx.doi.org/10.1214/ss/1177011136

Hu Z and Yang R-C (2013a). Improved statistical inference for graphical description and interpretation of genotype x environment interaction. *Crop Sci.* 53: 2400-2410 http://dx.doi.org/10.2135/cropsci2013.04.0218.

Hu Z and Yang R-C (2013b). A new distribution-free approach to constructing the confidence region for multiple parameters. *PLoS One* 8: e81179 http://dx.doi.org/10.1371/journal.pone.0081179.

Jeffreys H (1961). Theory of probability, Oxford: Clarendon Press.

Josse J, van Eeuwijk FA, Piepho HP and Denis JB (2014). Another look at Bayesian analysis of AMMI models for genotype-environment data. *J. Agric. Biol. Environ. Stat.* 19: 240-257 10.1007/s13253-014-0168-z.

Kelly AM, Smith AB, Eccleston JA and Cullis BR (2007). The accuracy of varietal selection using factor analytic models for multi-environment plant breeding trials. *Crop Sci.* 47: 1063-1070 http://dx.doi.org/10.2135/cropsci2006.08.0540.

Liu G (2001). Bayesian computations for general linear-bilinear models. Ph.D. diss., University of Kentucky, Lexington.

Meyer K (2009). Factor-analytic models for genotype x environment type problems and structured covariance matrices. *Genet. Sel. Evol.* 41: 21-31. http://dx.doi.org/10.1186/1297-9686-41-21

Ooms JCL (2009). The highest posterior density posterior prior for Bayesian model selection. Available at http://www.stat.ucla.edu/~jeroen/files/thesis5.pdf. Accessed Nov 12, 2013).

Perez-Elizalde S, Jarquin D and Crossa J (2011). A general Bayesian estimation method of linear-bilinear models applied to plant breeding trials with genotype x environment interaction. *J. Agric. Biol. Environ. Stat.* 17: 15-37. http://

dx.doi.org/10.1007/s13253-011-0063-9

Piepho HP (1997). Analyzing genotype-environment data by mixed models with multiplicative terms. *Biometrics* 53: 761-766. http://dx.doi.org/10.2307/2533976

R Development Core Team (2013). R: A language and environment for statistical computing. R Foundation for Statistical Computing, Vienna, Austria. Available at http://www.R-project.org/. Accessed June 12, 2014).

Raftery AE and Lewis S (1992). How many iterations in the Gibbs sampler? In: J.M. Bernardo, J.O. Berger, A.P. Dawid, and A.F.M. Smith, editors, Bayesian Statistics. Oxford Univ. Press, Oxford, UK. 763-773.

Rodrigues PC, Malosetti M, Gauch HG and van Eeuwijk FA (2014). A weighted AMMI algorithm to study genotype-by-environment interaction and QTL-by-environment interaction. *Crop Sci.* 54: 1555-1570. http://dx.doi.org/10.2135/cropsci2013.07.0462

Smith A, Cullis B and Thompson R (2001). Analyzing variety by environment data using multiplicative mixed models and adjustments for spatial field trend. *Biometrics* 57: 1138-1147 http://dx.doi.org/10.1111/j.0006-341X.2001.01138.x.

Smith AB, Ganesalingam A, Kuchel H and Cullis BR (2015). Factor analytic mixed models for the provision of grower information from national crop variety testing programs. *Theor. Appl. Genet.* 128: 55-72 http://dx.doi.org/10.1007/s00122-014-2412-x.

Stefanova K and Buirchell B (2010). Multiplicative mixed models for genetic gain assessment in lupin breeding. *Crop Sci.* 50: 880-891. http://dx.doi.org/10.2135/cropsci2009.07.0402

Thompson R, Cullis BR, Smith AB and Gilmour AR (2003). A sparse implementation of the average information algorithm for factor analytic and reduced rank variance models. *Aust. N. Z. J. Stat.* 45: 445-459. http://dx.doi.org/10.1111/1467-842X.00297

Viele K and Srinivasan C (2000). Parsimonious estimation of multiplicative interaction in analysis of variance using Kullback-Leibler information. *J. Stat. Plan. Inference* 84: 201-219 http://dx.doi.org/10.1016/S0378-3758(99)00151-2.

Yan W and Tinker NA (2006). Biplot analysis of multi-environment trial data: Principles and applications. *Can. J. Plant Sci.* 86: 623-645 http://dx.doi.org/10.4141/P05-169.

Yan W, Hunt LA, Sheng Q and Szlavnics Z (2000). Cultivar evaluation and mega-environment investigation based on GGE biplot. *Crop Sci.* 40: 597-605 http://dx.doi.org/10.2135/cropsci2000.403597x.

Yan W, Kang MS, Woods BMS and Cornelius PL (2007). GGE biplot *vs* AMMI analysis of genotype-by-environment data. *Crop Sci.* 47: 643-653 http://dx.doi.org/10.2135/cropsci2006.06.0374.

Yan W, Glover KD and Kang MS (2010). Comment on "Biplot analysis of genotype x environment interaction: Proceed with caution", by R.-C. Yang, J. Crossa, P.L. Cornelius, and J. Burgueño in 2009 49:1564-1576. *Crop Sci.* 50: 1121-1123 http://dx.doi.org/10.2135/cropsci2010.01.0001le.

Yang RC, Crossa J, Cornelius PL and Burgueño J (2009). Biplot analysis of genotype x environment interaction: Proceed with caution. *Crop Sci.* 49: 1564-1576 http://dx.doi.org/10.2135/cropsci2008.11.0665.

Supplementary material

S1 Table. Posterior means (GGEB), credible region (95% C.I., LL: Lower limit, UL: upper limit), and least squares estimates (GGEF) for the first two genotypic and environmental singular vectors.